Dynamic heterogeneity in an *E. coli* stress response regulon mediates gene activation and antimicrobial peptide tolerance

Caroline M. Blassick[1,2], Jean-Baptiste Lugagne[1,2], Mary J. Dunlop[1,2,+]

[1] Biomedical Engineering, Boston University, Boston, MA 02215, USA
[2] Biological Design Center, Boston University, Boston, MA 02215, USA
[+] corresponding author: mjdunlop@bu.edu

Abstract

The bacterial stress response is an intricately regulated system that plays a critical role in cellular resistance to drug treatment. The complexity of this response is further complicated by cell-to-cell heterogeneity in the expression of bacterial stress response genes. These genes are often organized into networks comprising one or more transcriptional regulators that control expression of a suite of downstream genes. While the expression heterogeneity of many of these upstream regulators has been characterized, the way in which this variability affects the larger downstream stress response remains hard to predict, prompting two key questions. First, how does heterogeneity and expression noise in stress response regulators propagate to the diverse downstream genes in their regulons. Second, when expression levels vary, how do multiple downstream genes act together to protect cells from stress. To address these questions, we focus on the transcription factor PhoP, a critical virulence regulator which coordinates pathogenicity in several gram-negative species. We use optogenetic stimulation to precisely control PhoP expression levels and examine how variations in PhoP affect the downstream activation of genes in the PhoP regulon. We find that these downstream genes exhibit differences both in mean expression level and sensitivity to increasing levels of PhoP. These response functions can also vary between individual cells, increasing heterogeneity in the population. We tie these variations to cell survival when bacteria are exposed to a clinically-relevant antimicrobial peptide, showing that high expression of the PhoP-regulon gene *pmrD* provides a protective effect against Polymyxin B. Overall, we demonstrate that even subtle heterogeneity in expression of a stress response regulator can have clear consequences for enabling bacteria to survive stress.

Introduction

Bacteria rely on complex, interconnected gene regulatory networks to maintain homeostasis and tolerate a diverse range of external stressors, including osmotic stress, heat or cold shock, nutrient starvation, acidic environments, and treatment with antimicrobial agents.[1,2] These environmental responses are often initiated by two-component systems, a set of critical regulators responsible for mediating responses to these stressors and triggers.[3–5] Receptors sense a stressor through direct ligand binding or other mechanisms, and the receptor's histidine kinase phosphorylates its response regulator, which then serves as a transcription factor to modulate downstream gene expression. These transcription factors may also directly or indirectly regulate other transcription factors, forming cascades that can consist of three or more levels.[6] Transcription factors in general may also act combinatorially, and many individual genes in these networks are regulated by a combination of two or more transcription factors.[7] Self-regulation in the form of positive or negative feedback is also a common motif, found in approximately 50% percent of transcription factors.[8] All of these properties add considerable complexity to bacterial regulatory networks. While extensive progress has been made in mapping these regulatory networks and developing models that predict the effect that perturbation of one gene will have upon others,[9,10] the precise relationship between the dynamics of a particular transcription factor and how it regulates genes within the stress response network is not always straightforward to determine.[11,12]

Additionally, transcription factors and other genes in stress response pathways can be heterogeneously expressed in isogenic populations, even in the absence of external stressors.[13,14] This heterogeneity can have

important functional consequences, for instance by enabling "bet-hedging" strategies that allow subsets of cells to survive stress or changes in environmental conditions.[15,16] This protective effect has also been implicated in the development of antibiotic resistance, by providing windows of tolerance in which cells have time to evolve more permanent resistance mechanisms.[17] These phenotypic consequences of expression heterogeneity highlight the importance of understanding the dynamics, extent, and sources of that heterogeneity. Fully characterizing stress response networks involves understanding the nature of heterogeneity in the network, how this heterogeneity can be propagated to other genes of the network, and what functional consequences this heterogeneity can have for the cell's ability to tolerate stress.

The PhoPQ stress response network has been well-studied due to its role in virulence in *Escherichia coli* and other gram-negative species, such as *Salmonella enterica* serovar Typhimurium and *Pseudomonas aeruginosa.*[18,19] PhoPQ is a two-component system consisting of the membrane-associated sensor PhoQ and its response regulator, PhoP. PhoQ can either phosphorylate or de-phosphorylate PhoP depending on environmental conditions. In non-activating conditions, the rate of phosphatase activity from PhoQ exceeds its kinase activity, and PhoP remains largely in an unphosphorylated state. In activating conditions, which include low Mg^{2+} or the presence of cationic antimicrobial peptides,[20] PhoQ phosphatase activity decreases, leading to an increase in the amount of phosphorylated PhoP. When phosphorylated, PhoP activates transcription from genes involved in a diverse range of functions, including Mg^{2+} transport, peptidoglycan recycling, outer membrane remodeling, and acid resistance.[21] While a relatively small number of promoters contain motifs annotated as PhoP binding boxes, deletion of PhoP results in the differential expression of over 600 genes.[22] The far-reaching effects of PhoP activation, both in terms of the number of genes affected and in the diversity of their functional roles, motivated our focus on the PhoP regulon to understand the role of differential regulation and heterogeneity across a stress response network.

Prior studies comparing measurements obtained from gel shift assays that were focused on promoters directly bound by PhoP have found that the affinity of PhoP for each of these promoters can differ.[21] These differences in affinity have been related to differences in the sequence and relative position of the PhoP binding motif. Intriguingly, PhoP overexpression data *in vivo* qualitatively disagree with these *in vitro* measurements. In one study, fluorescent reporters were used to track expression from several genes in the PhoP regulon over a range of stimulus levels. While the fold change in expression of each gene was similar over a range of Mg^{2+} concentrations, there were large differences in the baseline expression level of each gene, which span an order of magnitude between the genes with the lowest and highest expression levels.[23] Additionally, at higher expression levels of PhoP, such as those observed when cells are treated with an antimicrobial peptide, changes in PhoP activation resulted in differing expression patterns for each downstream gene. For instance, different downstream genes might have input-output relationships with different slopes, or have differing saturation points corresponding to where increased levels of PhoP result in no increases in downstream gene expression. These variable characteristics can help explain the differential regulation of genes that are all controlled by the same transcription factor. However, transcription factor binding affinity and saturation points alone are not the sole determinants of downstream response, thus a more comprehensive understanding of gene regulation via this pathway requires analysis of rich expression data in living cells.[24]

A number of strategies exist for characterizing gene networks in living cells, including the construction of gene knock-out strains which are then compared to wild-type cells.[25] However, many of these methods do not capture the full range of network dynamics or fail to capture cell-to-cell heterogeneity within a population. Static methods, such as gene knockout screens, inherently fail to capture the rich dynamics that underlie gene network regulation.[26] Dynamic perturbations, such as varying the amount of a given transcription factor over time, can capture more information than a single snapshot, and can additionally allow for the characterization of cell-to-cell heterogeneity or noise in gene expression.[27] While chemical induction may be used to modulate expression, it is limited by the fact that chemical inducers must be

introduced to cells through the culture medium. This makes it challenging to rapidly switch perturbation schemes or to subject cells to a wide range of perturbations.

Optogenetic, or light-based, regulation of gene expression provides a powerful alternative, offering superior spatial and temporal resolution.[28] Additionally, optogenetic regulation can be linked with hardware controllers for feedback-enabled control of the gene of interest, providing precise control over expression levels.[29] This makes optogenetic control an especially attractive option for obtaining rich, single-cell datasets with high reproducibility.

To examine the dynamics and cell-to-cell heterogeneity of the PhoP regulon, we leveraged the advantages of optogenetic control to modulate levels of PhoP. We then traced the effect of PhoP activity level to a suite of downstream genes using fluorescent reporters. In both bulk culture and at the single-cell level, we find marked differences in the activation patterns of different reporters. Precise optogenetic control and single-cell gene expression data also revealed new insights into the role that cell-to-cell heterogeneity plays in this important stress response network. Within each individual gene, we found broad consistency in the ways that populations of cells respond to the same stimulus. However, we uncovered subtle differences in the responsiveness of individual cells over time. The effects of these differences in responsiveness are critical, which we demonstrate by treating cells with the antimicrobial peptide Polymyxin B. We found that while the PhoP-controlled gene *pmrD* plays a role in resistance, this effect is not due strictly to high levels of PhoP activation alone. Rather, it is cells with high levels of responsiveness to PhoP activation, and thus relatively higher levels of *pmrD*, that have the greatest chance of survival. Importantly, we found that *pmrD* expression levels are more important than overall PhoP levels for determining a cell's survival. Altogether, our results demonstrate that variable input-output relationships between a stress response transcription factor and its regulon play an important role in shaping the dynamics and functional consequences of network activation. Furthermore, we showcase a powerful platform with which the dynamics and heterogeneity of regulatory pathways can be investigated at the single-cell level.

Results

Optogenetic system for control of gene activation

To enable rapid and precise control, we used an optogenetic platform for activation of PhoP. For real-time tracking of downstream network dynamics, we used PhoP-regulated gene reporters to examine the effect of PhoP perturbation on a diverse subset of its regulon. While there is evidence that PhoP can bind the promoters of downstream genes in an unphosphorylated (i.e., not activated) state,[30] it is most active when phosphorylated by the sensor kinase PhoQ under low Mg^{2+} conditions (Fig. 1A). PhoP then activates transcription of a set of genes with diverse functions. Of these genes, we investigated a subset that represents a broad range of these functions and has strong evidence of direct control via PhoP. Specifically, we selected *hemL*, a glutamate-1-semialdehyde aminotransferase involved in porphyrin biosynthesis;[31] *nagA*, an N-acetylglucosamine-6-phosphate deacetylase involved in peptidoglycan recycling;[32] *pmrD*, a homolog to a protein implicated in Polymyxin B resistance in *Salmonella enterica*;[33] *rstA*, a transcriptional regulator associated with virulence in pathogenic strains of *E. coli*;[34,35] *slyB*, a membrane lipoprotein important for maintaining membrane integrity during stress;[36] and *yrbL*, an uncharacterized protein previously found to be regulated by PhoP.[21] PhoP can additionally activate transcription from its own promoter in a form of positive autoregulation.[18]

The low Mg^{2+} conditions that result in maximal phosphorylation of PhoP can be severely growth limiting (Fig. S1), which complicates culturing and controlling cells. To circumvent this, we employed the strategy of Miyashiro et al. by using a mutated version of PhoP, which behaves as though constitutively phosphorylated.[23] Unless otherwise noted, it is this mutated version of PhoP that is used for all optogenetic

experiments. Additionally, for all optogenetic experiments, we used a Δ*phoP* strain to prevent confounding effects from variations in native *phoP* expression.

To enable precise control of PhoP dynamics, we employed the CcaS/R two-component optogenetic system.[37] In this system, the CcaS sensor kinase enters its active conformation upon exposure to green light (535 nm), allowing it to phosphorylate the CcaR response regulator. Phosphorylated CcaR then activates transcription from the optogenetic P_{cpcG2} promoter. Red light (670 nm) reverses this process, repressing transcription. We placed the PhoP transcription factor under the control of the P_{cpcG2} promoter, allowing its levels to be increased when cells were exposed to green light and decreased when cells were exposed to red light (Fig. 1B). To have a readout of transcription factor production, we also placed the gene encoding the red fluorescent protein mCherry under control of the P_{cpcG2} promoter. As a measure of downstream activation, we utilized a set of reporter plasmids,[38] which consists of the gene encoding green fluorescent protein GFP under the control of a promoter known to be regulated by PhoP. To confirm that CcaS/R activation does not have spurious, non-specific effects on cell transcription, we also included a constitutive promoter reporter as a negative control. This dual fluorophore setup allows signal propagation to be traced from the PhoP transcription factor to downstream genes by comparing the levels of mCherry and GFP. Using a suite of different GFP reporters, each under the promoter of a different gene driving GFP expression, reveals how identical upstream transcription factor dynamics can result in different expression patterns from downstream genes. Additionally, comparing individual cells containing identical reporters can provide insights into cell-to-cell heterogeneity in gene expression and its propagation.

Optogenetic control of PhoP

We began by optogenetically stimulating the PhoP light-controlled strains and measuring the corresponding change in fluorescence from each gene reporter (Fig. 1C). Using an optogenetic well plate equipped with red and green LEDs whose intensities can be independently controlled, we subjected cells containing the optogenetic PhoP system to a range of green light intensities.[39] After five hours of light exposure, we used flow cytometry to measure mCherry and GFP fluorescence for all cells. mCherry levels, which report the amount of PhoP induction, increase with increasing levels of green light stimulation, as expected, and showed comparable profiles across all experiments. While all reporters for downstream genes showed an increase in GFP as optogenetic stimulation levels (i.e., PhoP levels) increased, there were notable differences in the response patterns, as well as in the baseline expression levels of each gene. Some genes, such as *rstA*, reliably demonstrated increases commensurate with all levels of optogenetic stimulation; others, such as *phoP*, only exhibited expression increases at the highest levels of stimulation. These differences in activation dynamics result in differently shaped response curves when GFP levels are compared as a function of mCherry levels (Fig. 1D). Fits to a Hill function model confirm the wide diversity of response profiles that these downstream genes exhibit in response to identical PhoP signals (Fig. 1D, Table S1). Intriguingly, the *nagA* reporter strain showed very low baseline GFP fluorescence with no detectable increase upon increasing stimulation levels, despite strong evidence that the *nagA* promoter binds PhoP.[21] This may be because the *nagA* promoter is also strongly repressed by NagC in the absence of inducing levels of N-acetylglucosamine-6-PO_4.[40] As expected, the constitutive control exhibited minimal responses to increasing optogenetic stimulation.

Because heterogeneity in gene expression is especially important for stress response, we next examined variations in expression level within single cells using the flow cytometry data. Populations with similar mean fluorescence levels can have differing population distributions, indicating a wider set of responses to the same input. This would indicate that higher cell-to-cell heterogeneity is present in the population, as the distributions of cell outputs are broader given the same input. There may also be differences in the correlation between mCherry and GFP values for individual cells, demonstrating a difference in how reliably the target gene responds to a change in PhoP expression. If this metric is relatively low, it can help explain why there may be high cell-to-cell heterogeneity in the population, by indicating that PhoP (mCherry) and downstream gene (GFP) expression are not tightly linked (Fig. S2). We began by asking

whether the width of the distribution of gene expression changed with increasing stimulation levels, since noise in gene expression is known to decrease as the copy number of its regulators increases.[41] We quantified this using the coefficient of variation, which measures the standard deviation of the distribution divided by its mean. Despite differences in expression patterns, each reporter strain had broadly similar coefficients of variation for GFP across all stimulation levels (Fig. 1E). This suggests that at the levels of PhoP activation explored in this study, there is not a large difference in the noise in downstream gene expression between the lowest and highest levels of PhoP activation, potentially indicating that PhoP copy number is not the main contributor to cell-to-cell variation.

Next, we calculated the correlation coefficient between mCherry and GFP values for each individual cell. This metric distinguishes how tightly correlated the two values are, providing an indication, at the single-cell level, of how reliably changes in mCherry translate to changes in GFP. We observed clear differences between the various gene reporter strains (Fig. 1F). For some genes, such as *pmrD*, the correlation between mCherry and GFP remains roughly constant over various levels of induction. For others, such as *phoP*, the correlation grows with increasing mCherry levels, potentially indicating that other transcription factors play a role in regulating *phoP* expression until PhoP levels reach a threshold for positive autoregulation. Still other genes have correlation coefficients that level off with high levels of PhoP, indicating potential promoter saturation. A potential concern could be that these saturating levels of PhoP exceed what would be achieved under physiological conditions. To show that this is not the case, we grew wild-type cells in low Mg^{2+} media while measuring the fluorescence from a representative reporter, using *slyB* as an example. We verified that under these conditions, *slyB* fluorescence can be even higher than in our engineered strain (Fig. S3). Thus, our platform modulates PhoP stimulation levels within a physiologically relevant range.

Single-cell PhoP regulon dynamics

Dynamic phenotype switching or bet-hedging within heterogenous populations of cells can be an important strategy to enable subsets of the population to withstand diverse types of stress. To explore whether this is the case in the PhoP network, we next asked whether the dynamics of PhoP regulation differ among the diverse genes in the regulon, and whether there is substantial heterogeneity among individual cells. In order to answer these questions, we grew a subset of the reporter strains in the mother machine microfluidic device to enable single-cell resolution measurements over many generations of cell growth.[42] For these experiments, we focused on the reporters *phoP*, *pmrD*, *slyB*, and *yrbL*. We chose these reporters because they represent a diverse subset of the activation patterns observed in the bulk culture experiments, while also having similar baseline fluorescence levels, allowing them to be imaged under identical microscopy settings. We additionally included the constitutive reporter strain as a negative control.

Once cells were loaded into the mother machine, they were subjected to a five-minute loop that consisted of imaging in phase contrast, mCherry, and GFP channels, as well as optogenetic stimulation. Because the cells are trapped within individual chambers in the mother machine, we were able to use a digital micromirror device (DMD) to provide optogenetic stimulation separately to each individual chamber, allowing us to collect data for three levels of light stimulation within the same experiment (Fig. 2A). Each microscopy experiment began with four hours of red DMD stimulation applied to all cells to homogenize their expression levels. After hour four, cells were randomly divided into three subpopulations, each receiving a different level of optogenetic simulation: low, moderate, or high (Fig. 2B). After eight hours under these illumination conditions, all cells were returned to a low state with red DMD stimulations for the remainder of the experiment.

In contrast to the flow cytometry data conditions, where we subjected bulk cultures to varying levels of green light illumination using a plate-based device and then measured mCherry and GFP fluorescence at a single timepoint, in microscopy experiments fluorescence imaging occurs every five minutes. We found that the green light exposure from fluorescence imaging alone was sufficient to fully activate the CcaS/R optogenetic system, and that to achieve lower levels of expression we could use red light to repress

expression. In the low stimulation subpopulation, cells were subjected to repressing red light from the DMD every five minutes. In the high stimulation subpopulation, cells received no DMD stimulation. However, as the data in Figure 2 show, the same level of light induction can produce variable levels of CcaS/R activation. Therefore, to achieve a similar moderate level of CcaS/R activation in all cells, we employed our previously described Deep Model Predictive Control platform[43] (Fig. S4) to generate tailored DMD stimulation patterns for each cell, creating a constant level of CcaS/R activation and resulting in a constant mCherry objective of 1300 A.U.

This method of control allowed each reporter strain to have closely comparable mCherry levels over time, even when acquired in separate experiments (Fig. 2B). The median mCherry of the moderate stimulation population is very close to the set point for each experiment, and even without feedback control, the mCherry levels of the low and high objective population show good agreement between experiments. The three induction levels also have distinct activation dynamics. Without feedback control, the high objective population accumulates mCherry over time, and shows continued expression past the 12h timepoint when repressive light is applied. Similarly, the low objective population slowly increases over time, due to the slight activation associated with illumination for image acquisition. The control algorithm maintains the moderate objective, reached after five hours of controlled illumination, and mCherry also decays slowly after constant red light is applied to repress activation. These results demonstrate that we were able to achieve tight control over PhoP levels in individual cells over time, allowing us to place cells at low, medium, and high levels of expression.

All reporter strains also showed a corresponding increase in GFP activity upon stimulation of PhoP, with GFP levels rising the most for the *slyB* strain and the least for *yrbL* (Fig. 2B). As with the flow cytometry data, these results show a striking difference in sensitivity to PhoP levels across the different gene promoters, despite all being controlled by the same transcription factor. Low sensitivity for some genes, such as *yrbL*, may be explained by the early saturation point that was also noted in the bulk culture experiments. While it was possible to conduct bulk culture experiments in the absence of all light except a repressing red wavelength, microscopy experiments required imaging with multiple other wavelengths that partially overlap with the activation spectrum of CcaS/R. This results in a small amount of activation of PhoP and downstream genes even under red DMD illumination, resulting in less sensitivity for reporters such as *yrbL*.

Despite differences in sensitivity, each of the strains showed a strong relationship between optogenetic activation and downstream gene expression. Computing the cross correlations for each strain over time reveals that mCherry and GFP levels are highly correlated for all cells, achieving maximum values approaching 1 in most cases (Fig. 2C). While equal increases in mCherry will not produce identical changes in GFP across the reporters, the high correlations that we observe indicate that for any deviation from the mean mCherry fluorescence, promoter activity from each reporter gene is very likely to deviate in the same direction. This relationship holds true across all stimulation levels. In addition, the cross correlation can be used to quantify time delays between two signals. We found that the maximum correlation occurred at a time lag of 0 minutes, indicating that changes in PhoP are quickly propagated to the downstream genes. While changes in GFP should, in principle, slightly lag changes in mCherry, measurement constraints, such as the temporal resolution of data collection, prevent the precise determination of the time of signal propagation. Additionally, the longer maturation time of mCherry in comparison to the GFPmut2 variant used may reduce any apparent time lags.[38,44] However, these constraints are universal across all experiments, meaning cross correlations of the different gene reporters can be compared; we also note that these temporal correlations differ significantly from an unregulated constitutive control. These results indicate that there are no dramatic differences in response time between the tested PhoP regulon promoters, and that overall response times are short.

While the maximum value of the cross correlation is high for all reporters, this does not translate into identical response curves. Strains show response curves that are qualitatively similar to those obtained from bulk culture experiments (Fig. 2D). The response profiles do not qualitatively change across all time points in the experiment, indicating a highly consistent relationship between amounts of PhoP in the cell and the response from downstream promoters (Fig. S5). Additionally, swapping the PhoP family reporters for a constitutive reporter reveals minimal relationship between stimulation levels and GFP expression, demonstrating that the optogenetic platform is not introducing spurious changes in gene expression (Fig. S6). Overall, these results show that while each gene in the PhoP regulon may exhibit a differing response to PhoP activation, the average response profile for each stays consistent under a range of conditions. Thus, genes in the PhoP regulon generally have highly reliable changes in expression as a function of PhoP activation when averaged across cells within the population.

Variations in promoter responsiveness

Given the overall strength and consistency of the relationship between PhoP levels and downstream gene expression, we sought to take advantage of our rich temporal, single-cell data to determine whether subtle heterogeneity may be present in the way that the PhoP signal propagates to downstream genes. To do so, we computed the ratio of GFP to mCherry in each cell over time, which we refer to here as the "responsiveness" of a gene to PhoP activation, i.e. the magnitude of the response for each unit of active PhoP (Fig. 3A). For some reporters, such as *phoP* and *pmrD*, this responsiveness ratio stays relatively consistent over time and between all stimulation levels. For *yrbL*, however, a decrease in responsiveness occurs at higher stimulation levels. This is consistent with the dynamics noted in the Hill functions fitted to each bulk culture response profile; as overall induction level increases, each gene reaches a point where it leaves the linear range of the Hill response. From this point forward, responsiveness will be relatively low. More surprising, however, is the variation in responsiveness between individual cells. At hour 12 of the experiment, we plotted the responsiveness of each cell as a function of its level of mCherry (Fig. 3B). We observed a negative correlation across cells, as expected given the saturation effect observed at higher levels of mCherry, but the slope and distribution of this correlation varies for each gene. While most cells at a given mCherry level show similar responsiveness, variation is present for all genes. This is especially true for *slyB*, where a wide range of GFP expression levels can result from similar mCherry levels, especially when mCherry is low.

We suspected that the ability of cells to have different responsiveness from each other might also mean their responsiveness could vary over time. To examine the temporal patterns of cell responsiveness, we plotted the responsiveness for a randomly selected sample of 25 cells that received either the low (Fig. 3C), moderate (Fig. 3D), or high (Fig. 3E) stimulation levels. We see that across all stimulation levels, individual cells can vary by several fold in their responsiveness levels. These differences are persistent over time and are heterogeneous across cells, indicating they are unlikely to come from temporary image segmentation artifacts or technical noise. However, cells can also transition between low and high responsiveness states on the timescale of hours, indicating that responsiveness can also change for each cell over time. Because each cell serves as its own normalization control, these variations are also unlikely to come from global factors affecting overall transcription or protein accumulation, such as growth rate, or from variability in induction.

The *yrbL* case shows near universally low responsiveness at higher stimulation levels, which makes sense given the saturation shown by this reporter. For the remaining reporters, however, there is at least some level of variation in responsiveness at each stimulation level, indicating that subtle heterogeneity in the PhoP response is common across a range of genes and induction levels. This, coupled with the fact that variations in responsiveness can span multiple generations, means that heterogeneity in the PhoP regulon could play a role in determining cell phenotype across a range of conditions.

Role of PhoP and PmrD in Polymyxin B tolerance

The heterogeneity in gene expression of PhoP family genes poses interesting questions about how this variation can affect the ability of individual cells to tolerate stressors. For instance, if higher levels of PhoP expression provide protective effects against antimicrobial agents, populations of bacteria could use this as a strategy to enable subsets of cells to survive. We investigated the functional consequences of PhoP system activation by challenging cells with lethal concentrations of the antimicrobial peptide Polymyxin B. Polymyxin B is a short, cationic lipopeptide used to treat infections of gram-negative bacteria. Its strong bactericidal effect and efficacy against multidrug resistant bacteria make it an important drug in clinical settings.[45] Polymyxin B targets bacterial membranes as the primary mode of action, making outer membrane modifications the main strategy for resistance.[46] A homolog of the PhoP family gene *pmrD* is strongly implicated in Polymyxin B resistance in *Salmonella enterica*, where it plays a role in linking PhoP activation to activation of PmrAB, a two-component regulatory system responsible for membrane modification.[47] However, the role of *pmrD* in *E. coli* is less clearly defined. While *pmrD* was previously thought not to connect *phoPQ* and *pmrAB* expression in *E. coli,*[33] later studies found evidence that *pmrD* can activate *pmrA* under certain conditions, such as during high activation of PhoPQ.[48] Thus, the precise relationship between PhoP, expression of *pmrD,* and the effect of each gene in enabling Polymyxin B resistance, remain uncertain. In particular, we sought to characterize the extent to which PhoP can protect against Polymyxin B, and the likelihood that *pmrD* serves as a link between PhoP activation and Polymyxin B tolerance.

To investigate the role of *pmrD* in Polymyxin B resistance in *E. coli*, we observed cells containing the *pmrD* reporter in the mother machine before and after switching to media containing lethal concentrations of Polymyxin B (0.5 μg/mL). We again initiated high, medium, and low levels of PhoP activation, following a four hour equilibration period. Polymyxin B was added to the growth media starting at hour eight (Fig. 4A). In contrast to the previous set of experiments, this control strategy was maintained for the duration of the experiment. This resulted in populations with low, medium, and high levels of *pmrD* expression (Fig. 4B). We note that control accuracy was impacted after the addition of Polymyxin B, when cells begin to grow more slowly, filament, or die

Throughout the experiment, we tracked cell growth rate; we used this information to determine when growth ceased, at which point cells were classified as dead (Fig. 4C). We found that a subset of cells die in the hours prior to Polymyxin B exposure due to cell aging or spontaneous filamentation. After Polymyxin B exposure, cells die more quickly, with fewer than 20% of cells remaining alive by the end of the experiment. However, the population of cells controlled with the high expression objective died less rapidly than the low and moderate target populations, which had very similar death rates.

Because activation of PhoP leads to *pmrD* transcription, it can be difficult to disentangle the effects of each individual gene. We sought to investigate whether *pmrD* overexpression itself provides a protective effect against Polymyxin B, or whether Polymyxin B survival is linked to PhoP activation through some other mechanism. We divided the cells into quartiles based on time of death, with 1st quartile cells dying most quickly following Polymyxin B exposure and 4th quartile cells surviving the longest. For this analysis, we considered cells from all control objectives together, though metrics for cells within each individual level of stimulation were also recorded (Fig. S7-9).

We first asked whether cells with higher mCherry levels, and consequently higher PhoP levels, were more likely to withstand Polymyxin B exposure. Unexpectedly, the longest-surviving cells did not tend to have higher mCherry levels when Polymyxin B was introduced, indicating that PhoP levels alone are not enough to determine cell survival (Fig. 4D). Next, we looked at how GFP levels, which report *pmrD* levels, related to Polymyxin B survival. We found that GFP levels were elevated in the longest-surviving population of cells (Fig. 4E). These results can be explained by looking at the responsiveness ratio: while having high mCherry expression did not guarantee survival, having high responsiveness (and thus high *pmrD* for a given

value of PhoP) did confer an advantage (Fig. 4F). These results point strongly to *pmrD* specifically, and not some other aspect of the PhoP regulon, as providing the protective effect against Polymyxin B.

Investigating the single-cell distribution in the moments prior to Polymyxin B exposure reveals additional patterns for survival. While there is no significant difference in mCherry levels between cell populations at the time of Polymyxin B exposure (Fig. 4G), GFP levels were significantly higher in the longest-surviving population of cells compared to the shortest-surviving population, with this difference mostly driven by an increase in the number of cells with moderate (1000 – 2000 A.U.) levels of GFP (Fig. 4H). Responsiveness values were also significantly higher in the longest-surviving population of cells (Fig. 4I). Interestingly, the difference in responsiveness values was driven mainly by the reduced presence of cells with low (<0.2) responsiveness, rather than an enrichment in very highly responsive cells. Altogether, these results point to the important role of subtle variations in the propagation of signals within a gene network in determining outcomes under stress conditions. While high PhoP activation may help open the door to higher levels of *pmrD* expression, high PhoP activation by itself is not sufficient to protect cells from the antimicrobial peptide. A portion of cells with high PhoP activation still died upon Polymyxin B exposure, as did a portion of the cells with high *pmrD* levels. Instead, responsiveness also plays a role: cells with high levels of *pmrD* expression, given their level of PhoP, are the best equipped to survive. This is evidenced by the increasing median, as well the higher minimum threshold, of responsiveness in longer-surviving cells.

Discussion

While heterogeneity in the expression of stress response transcription factors has been characterized in a wide range of contexts, few studies have examined how this heterogeneity is then propagated to the downstream genes that enact stress tolerance. While all PhoP-regulon genes we tested increased in expression as PhoP levels increased, they exhibited a wide variety of response patterns. Different target genes required different amounts of PhoP for activation and had different fold-changes when maximally induced. We also found that, analogous to stress response genes which exhibit seemingly stochastic patterns of high and low activity over time and across populations of isogenic cells, individual cells may also exhibit differences in responsiveness of genes to variations in transcription factor levels. These results highlight the advantages of examining multiple genes in a pathway, especially when seeking to link heterogeneity in gene expression to functional outcomes such as survival.

Our results underscore related work showing the differential effect of identical PhoP levels upon a range of gene promoters in its regulon.[21,23,49] While these differences in responsiveness partly stem from differences in overall PhoP levels and the tendency of some promoters to saturate, the differences in responsiveness that we noted for cells at the same level of overall PhoP expression point to the role of noise or other intracellular factors in determining the PhoP response. Additionally, the normalization of GFP values to the mCherry values of each cell helps control for any factors that would globally perturb the cell's transcription rate.

We have shown that even subtle heterogeneity in PhoP regulon gene expression can have important consequences for cell survival. Our experiments indicate that in conditions of non-saturating PhoP activation, some cells can gain an edge for survival to the Polymyxin B stressor due to higher-than-average expression of *pmrD*. Part of the reason for this higher-than-average expression may be that *pmrD* can also be activated in a PhoP-independent manner, as has been shown in acidic conditions.[48] These results point to potential gene targets that could be disrupted in combination with Polymyxin B treatment, or tested in clinical isolates that show resistance to the antimicrobial peptide for further insight into resistance mechanisms.[50] Despite PhoP being the main regulator of a range of virulence traits, precision targeting of *pmrD* may prove more effective in characterizing or preventing Polymyxin B tolerance.

Possible extensions of this work include testing other functional outcomes of variations in PhoP activity, such as the ability of cells to withstand acid or osmotic stress or to tolerate exposure to other antimicrobial peptides, since PhoP is involved in coordinating a wide array of stress tolerance mechanisms. While we chose to focus on exploring the relationship between total PhoP activity on downstream promoters, alternate experimental setups could be used to further disentangle the role that native genetic feedback mechanisms play in the system, where both positive and negative feedback loops can exhibit variable behavior depending on the strength of PhoP regulon activation.[51–53] This could be accomplished by leaving the native *phoP* gene intact, incorporating methods for tracking PhoP phosphorylation dynamics in real-time,[54] or employing sophisticated feedback compensation techniques made possible by optogenetic control.[55] Protein-level accumulation of gene products in the PhoPQ regulon could also be examined, as this has been shown to lead to additional heterogeneity in the response of other systems.[56] Similar studies could also be carried out with other transcription factors implicated in cell stress to uncover broader patterns in gene regulation. Together, these studies will shed light on the complex and sometimes subtle ways in which heterogeneity in gene expression associated with stress response can impact cell survival or evasion of antimicrobial therapies.

Materials and Methods

Plasmid and strain development

All experiments were carried out using the *E. coli* BW25113 strain or its derivatives. The BW25113 Δ*phoP* knockout strain was sourced from the Keio collection.[57] For this strain, we excised the kanamycin resistance cassette using the pCP20 plasmid,[58] and the pCP20 plasmid was subsequently cured by growing cultures at 43°C overnight. To confirm curing of both kanamycin resistance and the pCP20 plasmid, we tested single colonies to verify sensitivity to both kanamycin and ampicillin. We constructed the variant of the *phoP* gene that was used in all experiments (unless otherwise noted) by introducing the point mutations described in Miyashiro et al.[23] This variant behaves as though constitutively phosphorylated. The BW25113 Δ*phoP*:PcpcG2-*phoP* and BW25113:PcpcG2-*tetR* strains were constructed using lambda red combination.[58] All cassettes were integrated into the locus downstream of the *nupG* gene, using the homology regions 5'-TCGTGTCCCGACAGGCACACAGACGGTTAGCCACTAATTA-3' and 5'-AAAAAAACGGGTCACCTTCTGGCGACCCGTTTTTCTTTGCG-3'.

All *GFPmut2* reporter plasmids were sourced from the collection developed by Zaslaver et al.[38] The reporter plasmid used in TetR control experiments described below (Fig. S10) consisted of pBbS2k with TetR excised and with the gene encoding mCherry replaced with *sfGFP*.[59] The constitutive reporter was constructed by replacing the promoter sequence with a modified version of the phage T7 A1 promoter (5' - TTATCAAAAAGAGTATTGTCTTAAAGTCTAACCTATAGGAAAATTACAGCCATCGAGAGGGAC ACGGCGAA - 3').

mCherry was expressed under the control of the P_{cpcG2} promoter from a separate plasmid, which consisted of the pSR58.6 plasmid with *mCherry* replacing *sfGFP*. This plasmid was transformed along with pNO286-3 and the relevant reporter plasmids into each strain. This resulted in a system with a high dynamic range of mCherry expression, which allowed it to serve as an easily measurable readout of system activation while TetR or PhoP were modulated at lower levels. pSR58.6 and pNO286-3 correspond to Addgene plasmids #63176 and #107746, respectively, from Jeffrey Tabor's lab.

Bulk culture optogenetic experiments

All bulk culture optogenetic experiments were carried out using an optoWELL-24 optogenetic well plate device (opto bioLabs GmbH). Overnight cultures were diluted 1:200 into fresh Luria Broth (LB) (Fisher) and 500 μL total volume was added to each well of a 24 well plate. The optoWELL-24 was programmed

with individual red (657 nm peak intensity) and green (519 nm peak intensity) light intensities for each well. Each well received red light at an intensity of 0.36 mW/cm^2, while green light varied in intensity from 0 – 0.208 mW/cm^2 as detailed in the figure legends. The well plate was placed inside the optoWELL-24 device, and the device was placed in a shaking incubator at 37°C and 250 rpm. After 5 hours, a BioTek Synergy H1M plate reader was used to measure optical density, GFP (485 nm excitation, 528 nm emission), and mCherry (580 nm excitation, 610 nm emission) for each well. Optical density was measured at 700 nm to reduce overlap with the mCherry emission spectrum. 5 µL was also sampled from each well and diluted into 145 µL of phosphate-buffered saline for flow cytometry using a GuavaFlow easyCyte HT flow cytometer. 5000 flow events were acquired for each sample. Flow cytometry data were gated to remove dead cells and cells with non-positive fluorescence values using the FlowCal package in Python. Fluorescence distributions were fit to a kernel density estimation curve using the Seaborn package in Python, with a grid size of 50.

Geometric means of fluorescence measurements for each reporter and light condition were used to fit a Hill equation:

$$GFP = \frac{A * mCherry^n}{k^n + mCherry^n} + B$$

The parameters A, k, n, and B were independently fit for each reporter strain using the curve_fit() function from the SciPy package in Python.[60] Fit values are listed in Table S1.

To validate that our optogenetic platform was not introducing spurious effects on expression from gene reporters, we performed additional bulk culture experiments using a synthetic gene inverter circuit. A *gfp* reporter was placed under control of the P_{Tet} TetR-repressible promoter, while the optogenetic CcaS/R system was used to control TetR repressor levels by placing the *tetR* gene and the *mCherry* gene downstream of the P_{cpcG2} promoter (Fig. S10A). We verified that increasing levels of green light stimulation resulted in increasing levels of mCherry, while GFP levels decreased (Fig. S10B). Overall, the system showed a consistent inverse relationship (Fig. S10C), adding confidence that our platform could detect input-output relationships.

Mother machine microfluidic device

Mother machine devices were produced as previously described.[14] Briefly, SU-8 resin molds were made via stereolithography based on the design available at https://gitlab.com/dunloplab/mother_machine. Polydimethylsiloxane (PDMS) (Dow Corning Sylgard 184) was poured into the molds, cured overnight at 75°C, and cut from the molds. Inlets and outlet holes were punched at either end of each channel using a 0.75 mm biopsy punch and the chip was plasma bonded to glass slides. Following binding, chips were returned to the 75°C incubator for an additional 24 hours before use.

Time-lapse microscopy

Overnight cell cultures were refreshed 1:100 into fresh LB medium and grown for 2-3 hours before being loaded into the mother machine microfluidic device. The device was spun at 5000 rpm for 3 minutes to load cells and then media tubing was connected at the inlet and outlet ports. LB supplemented with 2 g/L Pluronic F-127 (to reduce cell adhesion to the device) was supplied to the chip at a rate of 20 µL/min using a peristaltic pump. For all mother machine experiments, a concentration of 50 µg/mL chloramphenicol was provided as the sole antibiotic for plasmid maintenance. This concentration was selected to minimize cell stress while still preventing media contamination.

Cells were imaged with the following order and exposure times: phase contrast (50 ms), mCherry (35 ms), and GFP (50 ms). Following imaging, cells were either exposed to 100 ms of red light from a digital micromirror device (DMD) in order to repress CcaS/R activity, or they received no DMD stimulation.

Additionally, the full chip was exposed to low levels of constant red light from an Arduino-controlled NeoPixel Ring (Adafruit 1586) set to 25% maximum intensity, which was affixed directly above the microscope platform, in order to reduce the strength of background activation.

Deep model predictive control

For the moderate light exposure case, deep model predictive control was enacted on cells using the platform previously developed.[43] Unless otherwise specified, control parameters used were the same as in the original study. Briefly, snapshots of the cells were segmented and features such as fluorescence and cell length were extracted in real-time.[61] The features were fed into the deep model predictive control algorithm, which uses a trained model to predict which optogenetic stimulations are most likely to make the cell's mCherry fluorescence match the desired levels over time. The optimal optogenetic stimulations were used to create an image that was then loaded into the DMD to stimulate individual cells. We acquired a new training set for the prediction model by subjecting the optogenetic strains to random red stimulations using the DMD. Three experiments were conducted to acquire this training set, each tracking approximately ~2,000 cells over a period of at least 16 hours. Each training set contained cells with several different PhoP-responsive GFP reporter plasmids, although in principle the specific reporter used should not matter, because the model was not trained on GFP values and only uses mCherry fluorescence values.

Mother machine experiment data analysis

Cell segmentation and feature extraction were carried out on-the-fly during experiments using DeLTA software,[61] as previously described.[43] This provided data on fluorescence and cell area for each mother cell over the course of the experiment. Growth rate was calculated *a posteriori* from cell area data, according to the following formula:

$$Growth = \mu(t) = \frac{area(t+1) - area(t)}{area(t)}$$

To simplify analysis, cells experiencing division or non-physiological growth rates in any given frame (namely, rates < -0.2 hr^{-1} or > 0.3 hr^{-1}), which occasionally occurred due to segmentation algorithm glitches or cell death, were assigned "NaN" values. "NaN" values were also assigned to any objects identified by the segmentation algorithm whose total area was too small to represent a true cell. Growth rate data was then smoothed with a moving average filter over 5 frames to remove artefacts.

After growth rate was calculated over time for all cells, dead cells were filtered out from the dataset in order to draw conclusions based only on living cells, unless otherwise specified. Cells were removed if they had been assigned a "NaN" growth rate or a growth rate below 0.1 hr^{-1} for four consecutive frames. This metric was chosen to avoid removing cells which had only momentary slow growth or which experienced segmentation glitches for a small number of frames. Only cells which survived for the full length of the experiment were considered for analysis. For each experiment, at least 100 surviving cells were present for each reporter and stimulation condition.

Normalized cross correlations were calculated by using the NumPy function "np.correlate()", then dividing by the square root of the product of each signal's auto-correlation with itself.

Polymyxin B survival experiments

Polymyxin B survival experiments were carried out using a similar protocol for optogenetic stimulation, with the following differences: After the first four hours of red light DMD stimulation, the step-on control objectives were maintained for the full course of the experiment, rather than stepping-off at hour 12. Additionally, after hour 8, Polymyxin B Sulfate (MedChemExpress) was added to the cell media at a final concentration of 0.5 μg/mL. Instead of removing cells which did not survive for the full duration of the experiment from analysis, all cells were included in analysis for Figures 4A-C. For Figures 4D-I, cells were removed from consideration following the frame of their death.

Acknowledgements

We thank Dr. Razan Alnahhas and Dr. Virgile Andreani for helpful discussions. Dr. John Ngo and Dr. Heidi Klumpe provided useful input on the manuscript. This work was supported by NSF grants MCB-2324909 and MCB-2032357 and NIH grant R01AI102922 to MJD. CMB received support from the NSF Graduate Research Fellowship under grant DGE-1840990.

Author contributions

C.M.B and M.J.D. conceived and designed the study. J.-B.L. developed the optogenetic hardware and software platforms. C.M.B. performed experiments and conducted data analysis. C.M.B. and M.J.D. wrote the manuscript with input from J.-B.L.

Figures

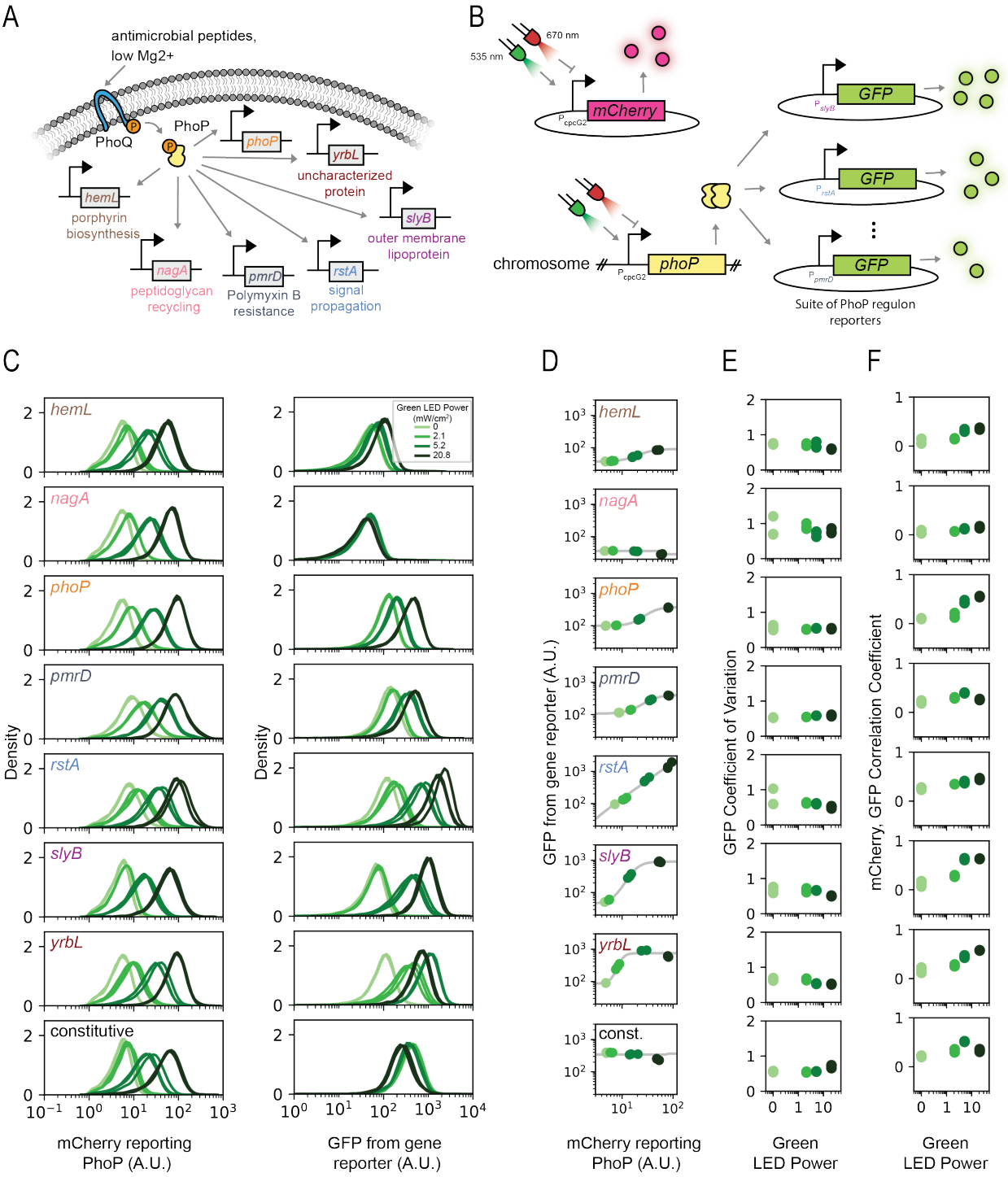

Figure 1. Optogenetic control of PhoP in bulk culture. (A) Schematic of the PhoPQ two-component system. Upon stimulation by low Mg^{2+} or the presence of antimicrobial peptides, there is a net increase in the rate of PhoP phosphorylation by the sensor kinase PhoQ. Phosphorylated PhoP activates transcription from a wide range of genes, a subset of which are included here. (B) Optogenetic regulation of PhoP. *phoP*, is placed downstream of the optogenetic P_{cpcG2} promoter along with mCherry. Increasing levels of green

light result in increased production of PhoP, which then activates transcription of *gfp* from PhoP-regulon reporter plasmids. (C) mCherry and GFP fluorescence distributions for cells containing the system described in panel B, under a range of green light stimulation levels. n = 3 technical replicates for each green light level. (D) Geometric means of GFP and mCherry fluorescence of the cells from panel C. Grey line represents best fit to a Hill function model. (E) Coefficient of variation for GFP across all cells. (F) Mean correlation coefficient between mCherry and GFP calculated across all individual cells.

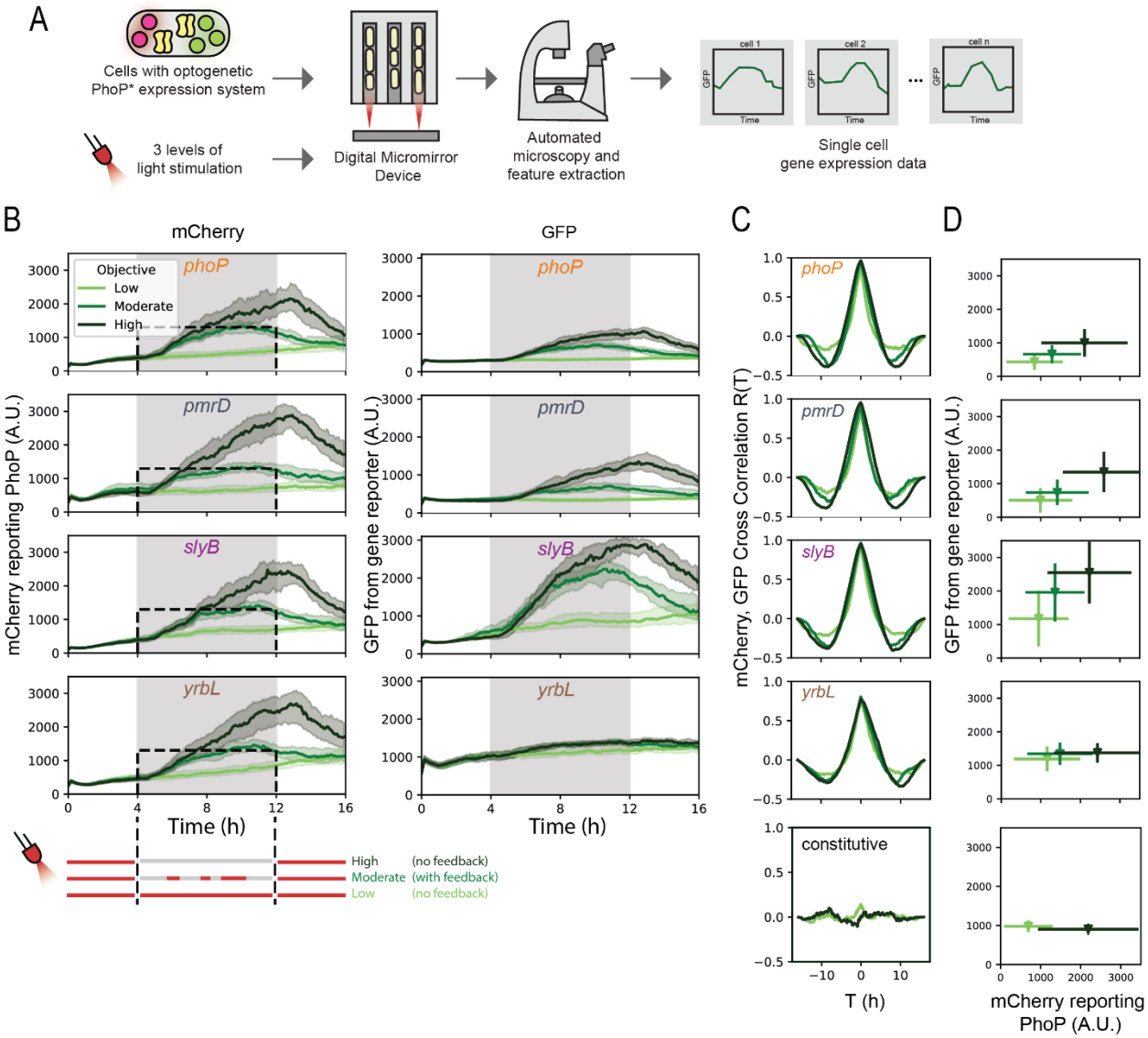

Figure 2. Single-cell optogenetic control of PhoP. (A) Experimental setup. Mother cells containing the PhoP optogenetic system are trapped in the end of the mother machine microfluidic device, allowing for long-term imaging. A Digital Micromirror Device provides individual stimulation to each mother machine chamber. Cells are imaged with automated microscopy and segmented on-the-fly, allowing for real-time monitoring of mCherry and GFP fluorescence. (B) mCherry and GFP expression levels over time for cells expressing optogenetically controlled PhoP. For the first and last four hours of each experiment, all cells receive red stimulation. Between hours 4 and 12, cells are randomly assigned to one of three stimulation conditions: low, which receives constant red stimulations; high, which receives no red stimulations; and moderate, which is controlled to maintain 1300 A.U. mCherry fluorescence levels. Median plus error bars representing the middle quintile are shown for each stimulation condition. n > 100 individual cells for each stimulation condition. (C) Median values of cross correlations computed between mCherry and GFP for every individual cell over time. Data for the constitutive control at low and high stimulation levels are also included. (D) Relationship between mean mCherry and GFP fluorescence across all cells at time t = 12 hours. Error bars represent standard deviation.

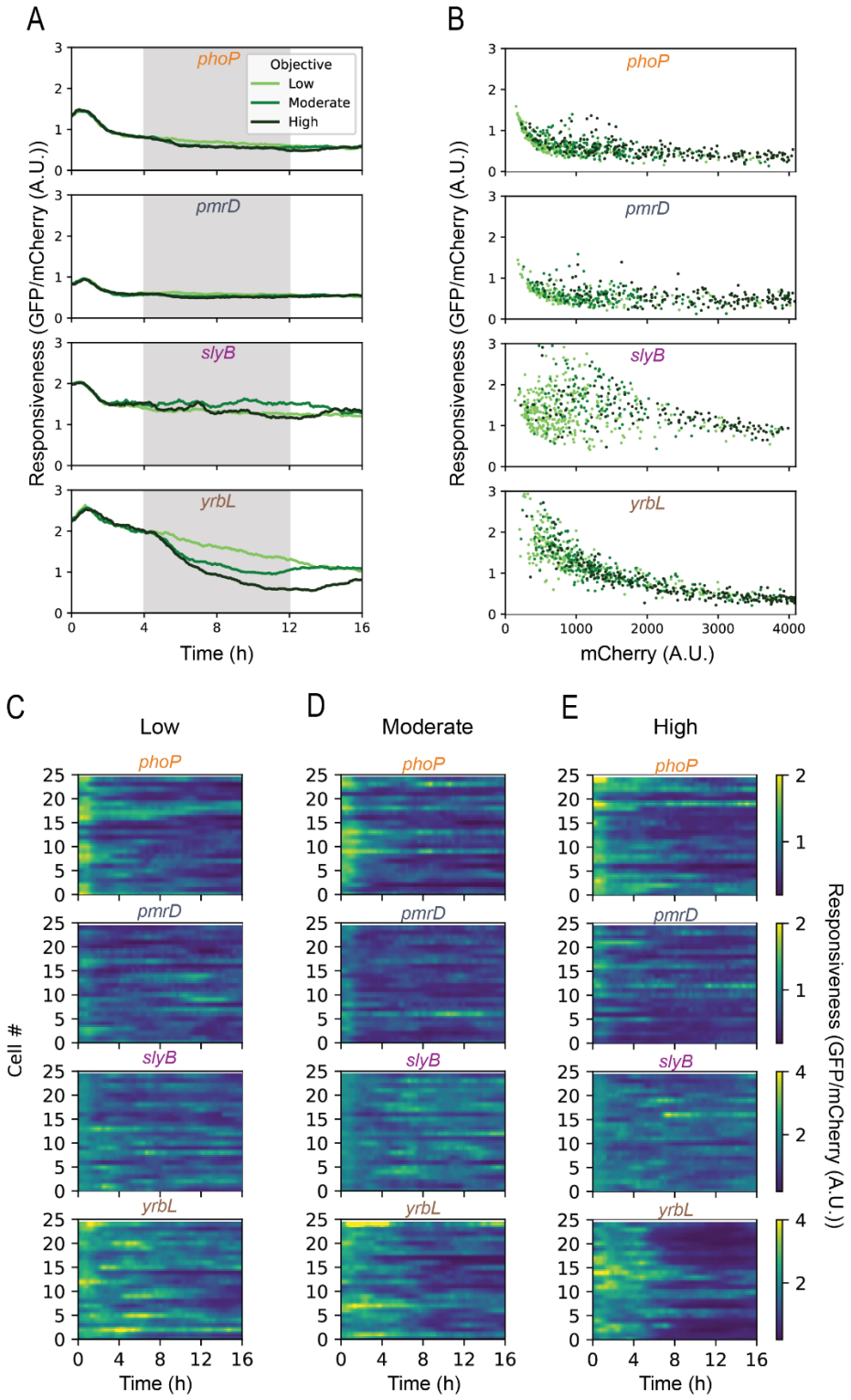

Figure 3. Heterogeneity in responsiveness to PhoP activation. (A) Median responsiveness, calculated as the ratio of GFP to mCherry for each cell, for each stimulation condition over time. (B) Scatter plot of responsiveness vs. mCherry level for individual cells at time t = 12 hours. (C-E) Responsiveness over time for individual cells in the low, moderate, and high stimulation conditions, respectively. A randomly sampled subset of 25 cells are displayed for each condition.

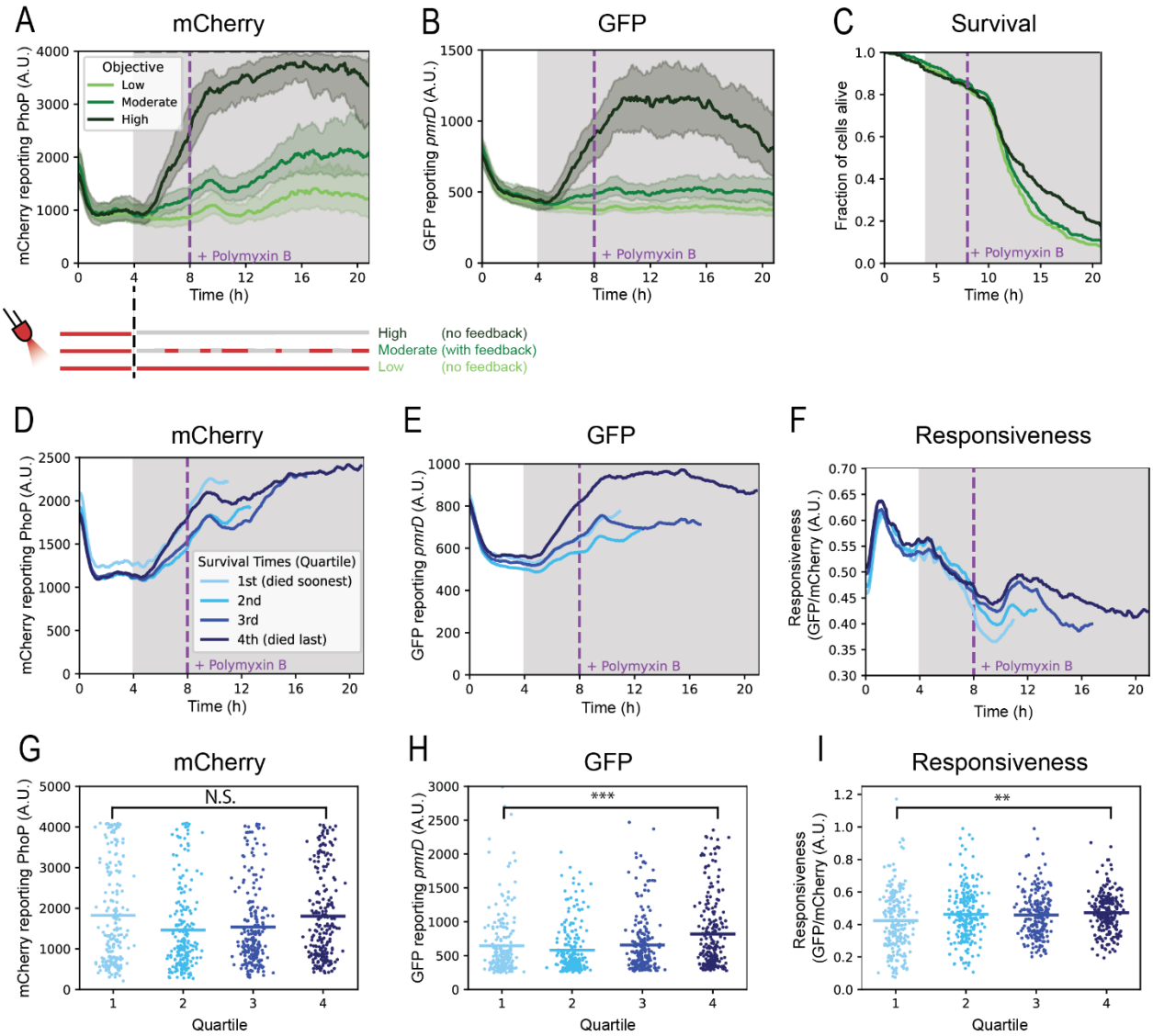

Figure 4. Role of *pmrD* in protecting cells from the antimicrobial peptide Polymyxin B. (A) mCherry reporting PhoP levels for all cells over time in low, moderate, and high stimulation regimens. The specified stimulation regimen begins at time t = 4 hours and continues until the end of the experiment. At time t = 8 hours, Polymyxin B is added to the cell media at a final concentration of 0.5 µg/mL. (B) GFP levels, from the *pmrD* reporter, for cells in each condition over time. Median plus middle quintile shown for each stimulation condition. (C) Fraction of cells remaining alive for each stimulation regimen over time. (D) Mean mCherry over time for cells from all stimulation regimes. Cells are partitioned into quartiles based on time of death after Polymyxin B exposure, with the 1st quartile representing the cells which died the most quickly and the 4th quartile representing cells which survived the longest. Note that the durations of the data traces vary between the four groups due to differences in time of death. (E) Mean GFP from the *pmrD* reporter over time for all cells. (F) Responsiveness, defined as GFP divided by mCherry, over time for all cells. (G) mCherry, (H) GFP, (I) and responsiveness values for individual cells in each survival quartile at t = 8 hours, just before the Polymyxin B is added. Horizontal bar represents population mean for

each quartile. N.S, not significant; ** = $P < 0.005$, *** = $P < 0.001$ in a two-sample t-test assuming unequal variance when comparing 1st and 4th quartile GFP values in the last timepoint before Polymyxin B addition. A single >3000 A.U. outlier cell is not depicted in plot (H), for visualization purposes, but was included in significance testing.

References

1. Martínez-Antonio, A., Janga, S. C. & Thieffry, D. Functional organisation of Escherichia coli transcriptional regulatory network. *J. Mol. Biol.* **381**, 238–247 (2008).
2. Abdelwahed, E. K., Hussein, N. A., Moustafa, A., Moneib, N. A. & Aziz, R. K. Gene Networks and Pathways Involved in Escherichia coli Response to Multiple Stressors. *Microorganisms* **10**, 1793 (2022).
3. Guo, M. S. & Gross, C. A. Stress-Induced Remodeling of the Bacterial Proteome. *Curr. Biol.* **24**, R424–R434 (2014).
4. Breland, E. J., Eberly, A. R. & Hadjifrangiskou, M. An Overview of Two-Component Signal Transduction Systems Implicated in Extra-Intestinal Pathogenic E. coli Infections. *Front. Cell. Infect. Microbiol.* **7**, 162 (2017).
5. Mizuno, T. Compilation of All Genes Encoding Two-component Phosphotransfer Signal Transducers in the Genome of Escherichia coli. *DNA Res.* **4**, 161–168 (1997).
6. Madan Babu, M. Evolution of transcription factors and the gene regulatory network in Escherichia coli. *Nucleic Acids Res.* **31**, 1234–1244 (2003).
7. Price, M. N. *et al.* Indirect and suboptimal control of gene expression is widespread in bacteria. *Mol. Syst. Biol.* **9**, 660 (2013).
8. Shen-Orr, S. S., Milo, R., Mangan, S. & Alon, U. Network motifs in the transcriptional regulation network of Escherichia coli. *Nat. Genet.* **31**, 64–68 (2002).
9. Ledezma-Tejeida, D., Ishida, C. & Collado-Vides, J. Genome-Wide Mapping of Transcriptional Regulation and Metabolism Describes Information-Processing Units in Escherichia coli. *Front. Microbiol.* **8**, 1466 (2017).
10. Faith, J. J. *et al.* Large-Scale Mapping and Validation of Escherichia coli Transcriptional Regulation from a Compendium of Expression Profiles. *PLoS Biol.* **5**, e8 (2007).

11. Ledezma-Tejeida, D., Altamirano-Pacheco, L., Fajardo, V. & Collado-Vides, J. Limits to a classic paradigm: most transcription factors in E. coli regulate genes involved in multiple biological processes. *Nucleic Acids Res.* **47**, 6656–6667 (2019).

12. Parisutham, V., Chhabra, S., Ali, M. Z. & Brewster, R. C. Tunable transcription factor library for robust quantification of regulatory properties in *Escherichia coli*. *Mol. Syst. Biol.* **18**, e10843 (2022).

13. Raj, A. & Van Oudenaarden, A. Nature, Nurture, or Chance: Stochastic Gene Expression and Its Consequences. *Cell* **135**, 216–226 (2008).

14. Sampaio, N. M. V., Blassick, C. M., Andreani, V., Lugagne, J.-B. & Dunlop, M. J. Dynamic gene expression and growth underlie cell-to-cell heterogeneity in *Escherichia coli* stress response. *Proc. Natl. Acad. Sci.* **119**, e2115032119 (2022).

15. Morawska, L. P., Hernandez-Valdes, J. A. & Kuipers, O. P. Diversity of bet-hedging strategies in microbial communities—Recent cases and insights. *WIREs Mech. Dis.* **14**, e1544 (2022).

16. Mitosch, K., Rieckh, G. & Bollenbach, T. Noisy Response to Antibiotic Stress Predicts Subsequent Single-Cell Survival in an Acidic Environment. *Cell Syst.* **4**, 393-403.e5 (2017).

17. Windels, E. M., Michiels, J. E., Van Den Bergh, B., Fauvart, M. & Michiels, J. Antibiotics: Combatting Tolerance To Stop Resistance. *mBio* **10**, e02095-19 (2019).

18. Groisman, E. A. The Pleiotropic Two-Component Regulatory System PhoP-PhoQ. *J. Bacteriol.* **183**, 1835–1842 (2001).

19. Monsieurs, P. *et al.* Comparison of the PhoPQ Regulon in Escherichia coli and Salmonella typhimurium. *J. Mol. Evol.* **60**, 462–474 (2005).

20. Yadavalli, S. S. *et al.* Antimicrobial peptides trigger a division block in Escherichia coli through stimulation of a signalling system. *Nat. Commun.* **7**, 12340 (2016).

21. Minagawa, S. *et al.* Identification and Molecular Characterization of the Mg2ƨ Stimulon of Escherichia coli. *J BACTERIOL* **185**, (2003).

22. Alteri, C. J., Lindner, J. R., Reiss, D. J., Smith, S. N. & Mobley, H. L. T. The broadly conserved regulator PhoP links pathogen virulence and membrane potential in *Escherichia coli*. *Mol. Microbiol.* **82**, 145–163 (2011).

23. Miyashiro, T. & Goulian, M. Stimulus-dependent differential regulation in the *Escherichia coli* PhoQ–PhoP system. *Proc. Natl. Acad. Sci.* **104**, 16305–16310 (2007).

24. Taverner, N. V., Smith, J. C. & Wardle, F. C. Identifying transcriptional targets. *Genome Biol.* (2004).

25. Tong, C. *et al.* Review of knockout technology approaches in bacterial drug resistance research. *PeerJ* **11**, e15790 (2023).

26. Castillo-Hair, S. M., Igoshin, O. A. & Tabor, J. J. How to train your microbe: methods for dynamically characterizing gene networks. *Curr. Opin. Microbiol.* **24**, 113–123 (2015).

27. Sampaio, N. M. V. & Dunlop, M. J. Functional roles of microbial cell-to-cell heterogeneity and emerging technologies for analysis and control. *Curr. Opin. Microbiol.* **57**, 87–94 (2020).

28. Lindner, F. & Diepold, A. Optogenetics in bacteria – applications and opportunities. *FEMS Microbiol. Rev.* **46**, fuab055 (2022).

29. Lugagne, J.-B. & Dunlop, M. J. Cell-machine interfaces for characterizing gene regulatory network dynamics. *Curr. Opin. Syst. Biol.* **14**, 1–8 (2019).

30. Lejona, S. *et al.* PhoP Can Activate Its Target Genes in a PhoQ-Independent Manner. *J. Bacteriol.* **186**, 2476–2480 (2004).

31. Ilag, L. L., Jahn, D., Eggertsson, G. & Söll, D. The Escherichia coli hemL gene encodes glutamate 1-semialdehyde aminotransferase. *J. Bacteriol.* **173**, 3408–3413 (1991).

32. Park, J. T. Identification of a Dedicated Recycling Pathway for Anhydro- *N* -Acetylmuramic Acid and *N* -Acetylglucosamine Derived from *Escherichia coli* Cell Wall Murein. *J. Bacteriol.* **183**, 3842–3847 (2001).

33. Winfield, M. D. & Groisman, E. A. Phenotypic differences between *Salmonella* and *Escherichia coli* resulting from the disparate regulation of homologous genes. *Proc. Natl. Acad. Sci.* **101**, 17162–17167 (2004).

34. Liu, Y. *et al.* RstA, a two-component response regulator, plays important roles in multiple virulence-associated processes in enterohemorrhagic Escherichia coli O157:H7. *Gut Pathog.* **11**, 53 (2019).

35. Gao, Q. *et al.* RstA is required for the virulence of an avian pathogenic Escherichia coli O2 strain E058. *Infect. Genet. Evol.* **29**, 180–188 (2015).

36. Janssens, A. *et al.* SlyB encapsulates outer membrane proteins in stress-induced lipid nanodomains. *Nature* **626**, 617–625 (2024).

37. Ong, N. T. & Tabor, J. J. A Miniaturized *Escherichia coli* Green Light Sensor with High Dynamic Range. *ChemBioChem* **19**, 1255–1258 (2018).

38. Zaslaver, A. *et al.* A comprehensive library of fluorescent transcriptional reporters for Escherichia coli. *Nat. Methods* **3**, 623–628 (2006).

39. Olson, E. J., Hartsough, L. A., Landry, B. P., Shroff, R. & Tabor, J. J. Characterizing bacterial gene circuit dynamics with optically programmed gene expression signals. *Nat Methods* **11**, (2014).

40. Plumbridge, J. A. Repression and induction of the *nag* regulon of *Escherichia coll* K-12: the roles of *nagC* and *nagA* in maintenance of the uninduced state. *Mol. Microbiol.* **5**, 2053–2062 (1991).

41. Elowitz, M. B., Levine, A. J., Siggia, E. D. & Swain, P. S. Stochastic Gene Expression in a Single Cell. *Science* **297**, 1183–1186 (2002).

42. Wang, P. *et al.* Robust Growth of Escherichia coli. *Curr. Biol.* **20**, 1099–1103 (2010).

43. Lugagne, J.-B., Blassick, C. M. & Dunlop, M. J. Deep model predictive control of gene expression in thousands of single cells. *Nat. Commun.* **15**, 2148 (2024).

44. Shaner, N. C. *et al.* Improved monomeric red, orange and yellow fluorescent proteins derived from Discosoma sp. red fluorescent protein. *Nat. Biotechnol.* **22**, 1567–1572 (2004).

45. Mohapatra, S. S., Dwibedy, S. K. & Padhy, I. Polymyxins, the last-resort antibiotics: Mode of action, resistance emergence, and potential solutions. *J. Biosci.* **46**, 85 (2021).

46. Zavascki, A. P., Goldani, L. Z., Li, J. & Nation, R. L. Polymyxin B for the treatment of multidrug-resistant pathogens: a critical review. *J. Antimicrob. Chemother.* **60**, 1206–1215 (2007).

47. Roland, K. L., Esther, C. R. & Spitznagel, J. K. Isolation and characterization of a gene, pmrD, from Salmonella typhimurium that confers resistance to polymyxin when expressed in multiple copies. *J. Bacteriol.* **176**, 3589–3597 (1994).

48. Rubin, E. J., Herrera, C. M., Crofts, A. A. & Trent, M. S. PmrD Is Required for Modifications to Escherichia coli Endotoxin That Promote Antimicrobial Resistance. *Antimicrob. Agents Chemother.* **59**, 2051–2061 (2015).

49. Zwir, I. *et al.* Dissecting the PhoP regulatory network of *Escherichia coli* and *Salmonella enterica*. *Proc. Natl. Acad. Sci.* **102**, 2862–2867 (2005).

50. Urban, C., Tiruvury, H., Mariano, N., Colon-Urban, R. & Rahal, J. J. Polymyxin-Resistant Clinical Isolates of *Escherichia coli*. *Antimicrob. Agents Chemother.* **55**, 388–389 (2011).

51. Miyashiro, T. & Goulian, M. High stimulus unmasks positive feedback in an autoregulated bacterial signaling circuit. *Proc. Natl. Acad. Sci.* **105**, 17457–17462 (2008).

52. Rao, S. D. & Igoshin, O. A. Overlaid positive and negative feedback loops shape dynamical properties of PhoPQ two-component system. *PLOS Comput. Biol.* **17**, e1008130 (2021).

53. Salazar, M. E., Podgornaia, A. I. & Laub, M. T. The small membrane protein MgrB regulates PhoQ bifunctionality to control PhoP target gene expression dynamics. *Mol. Microbiol.* **102**, 430–445 (2016).

54. Butcher, R. J. & Tabor, J. J. Real-time detection of response regulator phosphorylation dynamics in live bacteria. *Proc. Natl. Acad. Sci.* **119**, e2201204119 (2022).

55. Harrigan, P., Madhani, H. D. & El-Samad, H. Real-Time Genetic Compensation Defines the Dynamic Demands of Feedback Control. *Cell* **175**, 877-886.e10 (2018).

56. Wilson, M. Z., Ravindran, P. T., Lim, W. A. & Toettcher, J. E. Tracing Information Flow from Erk to Target Gene Induction Reveals Mechanisms of Dynamic and Combinatorial Control. *Mol. Cell* **67**, 757-769.e5 (2017).

57. Baba, T. *et al.* Construction of *Escherichia coli* K-12 in-frame, single-gene knockout mutants: the Keio collection. *Mol. Syst. Biol.* **2**, 2006.0008 (2006).

58. Datsenko, K. A. & Wanner, B. L. One-step inactivation of chromosomal genes in *Escherichia coli* K-12 using PCR products. *Proc. Natl. Acad. Sci.* **97**, 6640–6645 (2000).

59. Lee, T. S. *et al.* BglBrick vectors and datasheets: A synthetic biology platform for gene expression. *J. Biol. Eng.* **5**, 12 (2011).

60. Virtanen, P. *et al.* SciPy 1.0: fundamental algorithms for scientific computing in Python. *Nat. Methods* **17**, 261–272 (2020).

61. Lugagne, J.-B., Lin, H. & Dunlop, M. J. DeLTA: Automated cell segmentation, tracking, and lineage reconstruction using deep learning. *PLOS Comput. Biol.* **16**, e1007673 (2020).